180 min. All reactions were conducted in 100 μl of 10 mM Hepes (pH 7.5) at 37°C. Cleavage products were analyzed with a Waters high-performance liquid chromatograph and DEAE column using a gradient elution of 50 mM ammonium phosphate (pH 5.2) to 450 mM ammonium phosphate (pH 5.7) (*6*). PKCI hydrolysis reactions were conducted as above with ADP, AppA, and ATP as substrates. AppA hydrolysis was qualitatively observed for PKCI, as was 7-methyguanosine 5′-triphospho-5′-adenosine and Ap_5A hydrolysis for FHIT.

9. Y. F. Wei and H. R. Matthews, *Methods Enzymol.* **200**, 388 (1991); S. J. Pilkis *et al.*, *J. Biol. Chem.* **258**, 6135 (1983); C. A. Hasemann, E. S. Istvan, K. Uyeda, J. Deisenhofer, *Structure* **4**, 1017 (1996); Z. B. Rose, *Methods Enzymol.* **87**, 42 (1982); S. H. Thrall, A. F. Mehl, L. J. Carroll, D. Dunaway-Marino, *Biochemistry* **32**, 1803 (1983); S. Morera, M. Chiadmi, G. LeBras, I. Lascu, J. Janin, *ibid.* **34**, 11062 (1995); J. E. Wedekind, P. A. Frey, I. Rayment, *ibid.* **35**, 11560 (1996).
10. FHIT protein (5 μg) was incubated in 100-μl reactions with 50 μM unlabeled ATP spiked with 0.033 μM [α-^{32}P]ATP (~3000 Ci/mmol) or with 0.033 μM [2,8-^{3}H]ATP (25 to 40 Ci/mmol). The reaction was stopped after 60 min by precipitation and denaturation by addition of 10% trichloroacetic acid (TCA) [bovine serum albumin (0.5 μg/μl) as carrier]. The pellet was resuspended in 0.1 N NaOH, reprecipitated with 10% TCA, and finally resuspended in 100 mM ammonium bicarbonate, pH 9 (*9*). The reaction was boiled in SDS sample buffer and loaded onto a 17.5% SDS–polyacrylamide gel electrophoresis (PAGE) gel for analysis. The radioactive bands in Fig. 4 were detected by film autoradiography over 6 hours (α-^{32}P) and 12 weeks (2,8-^{3}H). A similar approach was used to trap covalent phosphotyrosine intermediates in topoisomerase reactions [Y.-C. Tse-Dinh, K. Kirkegaard, J. Wang, *J. Biol. Chem.* **255**, 5560 (1980)]. Radioactive labeling was coincident with the position of FHIT in SDS-PAGE.
11. $R_{sym} = \Sigma|I - \langle I\rangle|/\Sigma I$, where I = observed intensity and $\langle I\rangle$ = average intensity; the crystallographic R factor is based on 95% of the data used in refinement and R_{free} is based on 5% of the data withheld for the cross-validation test. Unique reflections distinguish Bijvoet mates. All other statistics on refinement and diffraction data can be found in the respective PDB entries (codes: 4FIT, 5FIT, 6FIT, 1KPE, 1KPF, and 1AV5). FHIT and PKCI protein expression and purification were as described (*2, 3*). Crystallization of the various complexes is described in the PDB entries. The FHIT–AMP-CP complex was collected and processed at the Advanced Photon Source (APS) Structural Biology Center (SBC) undulator beamline 19-ID on the charge-coupled device detector [E. M. Westbrook and I. Naday, *Methods Enzymol.* **276**, 244 (1997); M. L. Westbrook, T. A. Coleman, R. T. Daley, J. W. Pflugrath, in *Proceedings of IUCr Computing School*, P. E. Bourne and K. Watenpaugh, Eds. (SDSC Inc., San Diego, CA, 1996)]. The FHIT adenosine-tungstate data were collected at the NSLS beamline X4A at the peak of the LII edge of tungsten in order to optimize the anomalous signal from the bound tungstate. All other data were collected on a RAXISII and processed with the programs DENZO and SCALEPACK [Z. Otwinowski and W. Minor, *Methods Enzymol.* **276**, 307 (1997)]. Subsequent data reduction was done with the CCP4 suite of programs [SERC (UK) Collaborative Computing Project 4 (Daresbury Laboratory, Warrington, UK, 1979)]. Although five of the reported structures all crystallized in previously reported space groups (*2, 3*), the PKCI-AMP complex crystallized in an alternative space group ($P4_32_12$) and was solved using a partial model (*3*) in molecular replacement with AMORE [J. Navaza, *Acta Crystallogr.* **A50**, 157 (1994)] and modeled with the program O [T. A. Jones, J. Y. Zou, S. W. Cowan, M. Kjeldgaard, *ibid.* **A47**, 110 (1991)]. Isomorphous, related space groups were solved by a similar approach in AMORE. All models were refined with X-Plor using the cross-validation test [A. T. Brünger, J. Kuriyan, M. Karplus, *Science* **235**, 458 (1987); A. T. Brünger, *Nature* **355**, 472 (1992)]. Each FHIT model roughly includes residues 2 to 108 and 125 to 147. Each PKCI model roughly includes residues 14 to 126. Occupancies for the α and β tungstate molecules refined to 0.50 and 0.54, respectively, for PKCI and to 0.47 for FHIT.
12. Vanadate and molybdate pentacovalent metal sites were identified in structures of chloroperoxidase, rat acid phosphatase, bovine low–molecular weight phosphotyrosyl phosphatase, ribonuclease A, and a vanadate-ADP transition-state complex of S1 myosin [B. Borah *et al.*, *Biochemistry* **24**, 2058 (1985); Y. Lindqvist, G. Schneider, P. Vihko, *Eur. J. Biochem.* **221**, 139 (1994); A. Messerschmidt and R. Wever, *Proc. Natl. Acad. Sci. U.S.A.* **93**, 392 (1996); C. A. Smith and I. Rayment, *Biochemistry* **35**, 5404 (1996); A. Wlodawer, M. Miller, L. Sjolin, *Proc. Natl. Acad. Sci. U.S.A.* **80**, 3628 (1983); M. Zhang, M. Zhou, R. L. Van Etten, C. V. Stauffacher, *Biochemistry* **36**, 15 (1997)]. The active sites of PKCI and FHIT share several structural similarities and characteristics with protein phosphatases, particularly rat acid phosphatase. A search of the small-molecule database revealed a pentacovalent tungstate structure with similar characteristics to those observed in our enzyme complex [I. Feinstein-Jaffe, J. C. Dewan, R. R. Schrock, *Organometallics* **4**, 1189 (1985)]. The bond lengths and angles observed in our crystal structures are in agreement with those observed in several other tungsten-containing molecules found in the database. We know of no reported protein structure that describes a similar pentacovalent tungstate complex.
13. L. Holm and C. Sander, *Structure* **15**, 165 (1997); *Trends Biochem. Sci.* **22**, 116 (1997).
14. J. E. Wedekind, P. A. Frey, I. Rayment, *Biochemistry* **34**, 11049 (1995).
15. S. V. Evans, *J. Mol. Graphics* **11**, 134 (1993).

16. We thank the staffs of beamline X4A at the National Synchrotron Light Source (NSLS) and beamline 19-ID at the APS. We particularly thank members of the Hendrickson lab for helpful discussion, and especially C. Bingman for discussions about catalysis. We also thank the Pyle, McDermott, and Parkin labs for helpful discussions and for use of resources during the analysis of the catalytic intermediate. Beamline X4A at the NSLS, a U.S. Department of Energy facility, is supported by the Howard Hughes Medical Institute. Use of the APS was supported by the U.S. Department of Energy, Basic Energy Sciences, Office of Energy Research. The SBC is supported by the U.S. Department of Energy, Office of Health and Environmental Research, Office of Energy Research. Both the SBC and APS are supported under contract W-31-109-ENG-38. This work was supported in part by National Cancer Institute training grant T32CA09503 (M.G.K.) and by a Helen Hay Whitney Foundation Fellowship to C.D.L.

3 April 1997; accepted 4 September 1997

Angiogenic and HIV-Inhibitory Functions of KSHV-Encoded Chemokines

Chris Boshoff,* Yoshio Endo, Paul D. Collins, Yasuhiro Takeuchi, Jacqueline D. Reeves, Vicki L. Schweickart, Michael A. Siani, Takuma Sasaki, Timothy J. Williams, Patrick W. Gray, Patrick S. Moore, Yuan Chang, Robin A. Weiss

Unique among known human herpesviruses, Kaposi's sarcoma–associated herpesvirus (KSHV or HHV-8) encodes chemokine-like proteins (vMIP-I and vMIP-II). vMIP-II was shown to block infection of human immunodeficiency virus–type 1 (HIV-1) on a CD4-positive cell line expressing CCR3 and to a lesser extent on one expressing CCR5, whereas both vMIP-I and vMIP-II partially inhibited HIV infection of peripheral blood mononuclear cells. Like eotaxin, vMIP-II activated and chemoattracted human eosinophils by way of CCR3. vMIP-I and vMIP-II, but not cellular MIP-1α or RANTES, were highly angiogenic in the chorioallantoic assay, suggesting a possible pathogenic role in Kaposi's sarcoma.

Kaposi's sarcoma (KS) is a highly angiogenic multicentric tumor most commonly seen in immunodeficient individuals. Since the acquired immunodeficiency syndrome (AIDS) epidemic, KS has become one of the most common tumors in parts of Africa and is the most common tumor found in HIV-infected individuals (*1*). Compared to classic KS found in patients from Mediterranean or East European descent, KS in AIDS patients is a more fulminant disease: The angiogenic properties of the HIV-1 Tat protein have been proposed to enhance KS tumor formation (*2*).

KSHV DNA is present in all KS biopsies, and antibodies to this virus are detectable mainly in those with KS or at risk of developing KS (*3*). These data, and previous epidemiological data indicating that an infectious agent is involved in KS pathogenesis (*4*), suggest that KSHV is likely to

C. Boshoff, Y. Takeuchi, J. D. Reeves, R. A. Weiss, Institute of Cancer Research, Chester Beatty Laboratories, London SW3 6JB, UK.
Y. Endo and T. Sasaki, Department of Experimental Therapeutics and Development Center for Molecular Target Drugs, Cancer Research Institute, Kanazawa University, Japan.
P. D. Collins and T. J. Williams, Department of Applied Pharmacology, Imperial College School of Medicine at National Heart and Lung Institute, London SW3 6LY, UK.
V. L. Schweickart and P. W. Gray, ICOS, 22021 20th Avenue Southeast, Bothell, WA 98021, USA.
M. A. Siani, Gryphon Sciences, San Francisco, CA 94080, USA.
P. S Moore and Y. Chang, Department of Pathology and Epidemiology, College of Physicians and Surgeons of Columbia University, New York, NY 10032, USA.
*To whom correspondence should be addressed.

play a central role in KS tumorigenesis. In KS biopsies, KSHV is present in most of the tumor cells (so-called spindle cells) and in endothelial cells (5). Although it appears that KSHV gene expression in most of these cells is restricted to latent genes (5), a proportion of endothelial and spindle cells in KS lesions harbor hundreds of viral particles, suggesting that lytic viral infection may be necessary to drive KS lesion formation (6) and the vMIPs are expressed in KS lesions (7). KSHV is also etiologically linked to multicentric Castleman's disease (MCD), a polyclonal lymphoproliferation associated with prominent vascularity (8).

Sequencing of the KSHV genome has demonstrated colinearity and similarity with the gamma-oncogenic viruses Epstein-Barr virus (EBV) and herpesvirus saimiri (HVS) (9). However, unique among known human herpesviruses, KSHV encodes two genes whose products show sequence similarity to the human CC chemokine family, with highest similarity to macrophage inflammatory protein–1α (MIP-1α) and RANTES: vMIP-I [open reading frame (ORF) K6] exhibits 37.9% amino acid sequence identity and vMIP-II (ORF K4) 41.1% amino acid identity to MIP-1α (*10*). The amino acid identity between vMIP-I and vMIP-II is 48%, and they are more closely related to each other phylogenetically than to cellular chemokines, suggesting that they have evolved by gene duplication within the virus genome rather than by independent acquisition from the host genome. A third KSHV ORF (K4.1) is also related to the CC chemokine family, but this gene is more distantly related and probably derived independently from another member of the CC chemokine family (*9*, *11*). Both vMIP-I and vMIP-2 are expressed in latently infected lymphoma cells, and their expression is induced by phorbol esters (*10*).

Chemoattractant cytokines (chemokines) and their receptors play a fundamental role in leukocyte migration and activation and in hematopoiesis (*12*). The finding that chemokine receptors act as cofactors for HIV-1 entry into $CD4^+$ cells and that the CC chemokines (MIP-1α, MIP-1β, RANTES, and eotaxin) can suppress some strains of HIV replication in peripheral blood mononuclear cells (PBMCs) and chemokine receptor–transfected cell lines has intensified interest in these proteins (*13*). vMIP-I can inhibit infection of some primary non–syncytium-inducing (NSI) HIV strains when cotransfected with CCR5, the recently identified coreceptor for NSI HIV-1 strains (*10*). We generated synthetic proteins (*14*) of vMIP-I and vMIP-II and assessed their capacity to inhibit HIV infection, induce calcium mobilization, and induce angiogenesis.

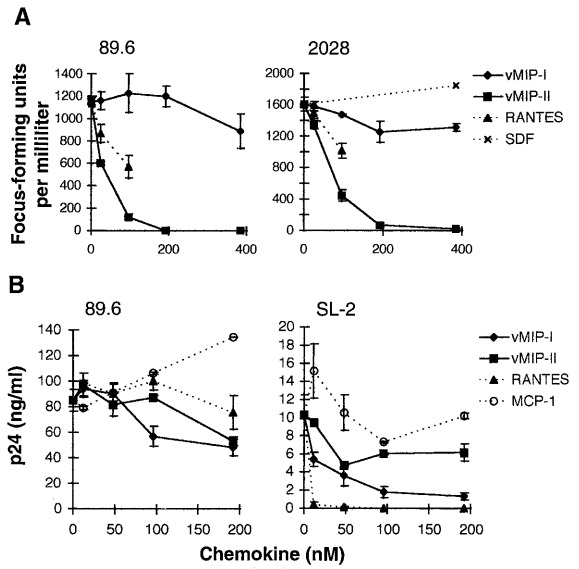

Fig. 1. Inhibition of HIV replication by vMIP-I and vMIP-II. (**A**) U87/CD4 cells stably expressing CCR3 were treated with the chemokines vMIP-I, vMIP-II, RANTES, and SDF at the concentrations indicated. Treated cells were challenged with the SI dualtropic HIV-1 strains 89.6 and 2028. Cells were fixed and immunostained for in situ p24 5 days later. p24-positive foci were counted, and average titers are shown. (**B**) PBMCs were challenged with 89.6 and NSI SL-2 HIV-1 strains in the absence or presence of chemokines vMIP-I, vMIP-II, RANTES, and MCP-1 at the concentrations indicated. Cell supernatants were harvested 9 days later and p24 levels measured. Average p24 concentrations are shown. Bars represent the standard error from triplicate wells. The results are representative of two and three separate experiments for strains 89.6 and SL-2, respectively.

We investigated whether vMIP-I and vMIP-II can suppress HIV-1 replication in U87/CD4 cells (a human glioma cell line) expressing HIV-1 coreceptors and in primary PBMCs (*15*). To define which chemokine receptors were most important for inhibition of HIV-1 infection by the vMIPs, we tested U87/CD4 cells stably expressing either CXCR4, CCR3, or CCR5 with the NSI strains SL-2 and SF162 and the dualtropic syncytium-inducing (SI) strains 89.6 and 2028. SL-2 and SF162 are primary NSI, macrophage-tropic strains that use the RANTES, MIP-1α, and MIP-1β receptor CCR5 to gain entry into $CD4^+$ cells. Strains 89.6 and 2028 are SI dual-tropic and can use CXCR4 and CCR3 in addition to CCR5 for entry. CD4-independent infection of an HIV-2 strain, ROD/B, on U87 cells expressing CXCR4 but not CD4 was also examined (*16*). Whereas modest levels of inhibition were observed with vMIP-II on infection of dual-tropic HIV-1 strains by way of CCR5 and CXCR4 as well as on HIV-2 ROD/B by way of CXCR4 (*17*), vMIP-II potently inhibited both 89.6 and 2028 infection, with geater than 95% inhibition at 200 nM on cells stably expressing CCR3 (Fig. 1A). No significant blocking of HIV infection by way of CCR3, CCR5, or CXCR4 on U87/CD4 cells by vMIP-I was observed (Fig. 1A) (*17*). These results suggest that vMIP-II binds predominantly to CCR3, rather than CXCR4 or CCR5. Alternatively, HIV-1 infection by way of CCR3 may be especially sensitive to chemokine inhibition.

We next tested whether vMIP-I or vMIP-II inhibited HIV-1 infection of PBMCs. Strains 89.6 and SL-2 were used in these studies. Both vMIP-I and vMIP-II partially inhibited SL-2 infection of PBMCs (Fig. 1B). Whereas RANTES reduced SL-2 infection of PBMCs by more than 98% at 12.5 nM, vMIP-I and vMIP-II were much less efficient, blocking infection by ~80% and 40%, respectively, at 100 nM. No substantial inhibition of 89.6 infection was observed. vMIP-I inhibited the CCR5-using SL-2 strain on PBMCs but not on $CCR5^+$ U87/CD4 cells. CCR5, however, is likely to be expressed at substantially lower levels on PBMCs than on cell lines such as U87/CD4. This difference may explain such differential cell type–dependent sensitivity to chemokine inhibition.

Because the HIV inhibition studies indicated that vMIP-II binds predominantly to CCR3, the eotaxin receptor, we investigated the potential of the vMIPs to act as agonists on CCR3. Because CCR3 is expressed predominantly on eosinophils (*18*), we used an in vitro human eosinophil activation assay that measures intracellular Ca^{2+} mobilization (*19*). vMIP-II, like eotaxin, was a potent activator of human eosinophils and was more active than MIP-1α or RANTES (Fig. 2A). In comparison, vMIP-II had no effect on Ca^{2+} flux in human neutrophils, whereas the CXC chemokines interleukin-8 (IL-8) and GROα were potent agonists (Fig. 2A). Despite the sequence similarities between vMIP-I and vMIP-II, vMIP-I was inactive on both eosinophils and neutrophils. We therefore examined whether vMIPs function as receptor antagonists on eosinophils and neutrophils, as has been demonstrated for synthetic NH_2-terminal variants of CC (for example, Met-RANTES) and CXC (for example, $IL\text{-}8_{1-69}$) chemokines (*20*). vMIP-I had no inhibitory effect on the response of eosino-

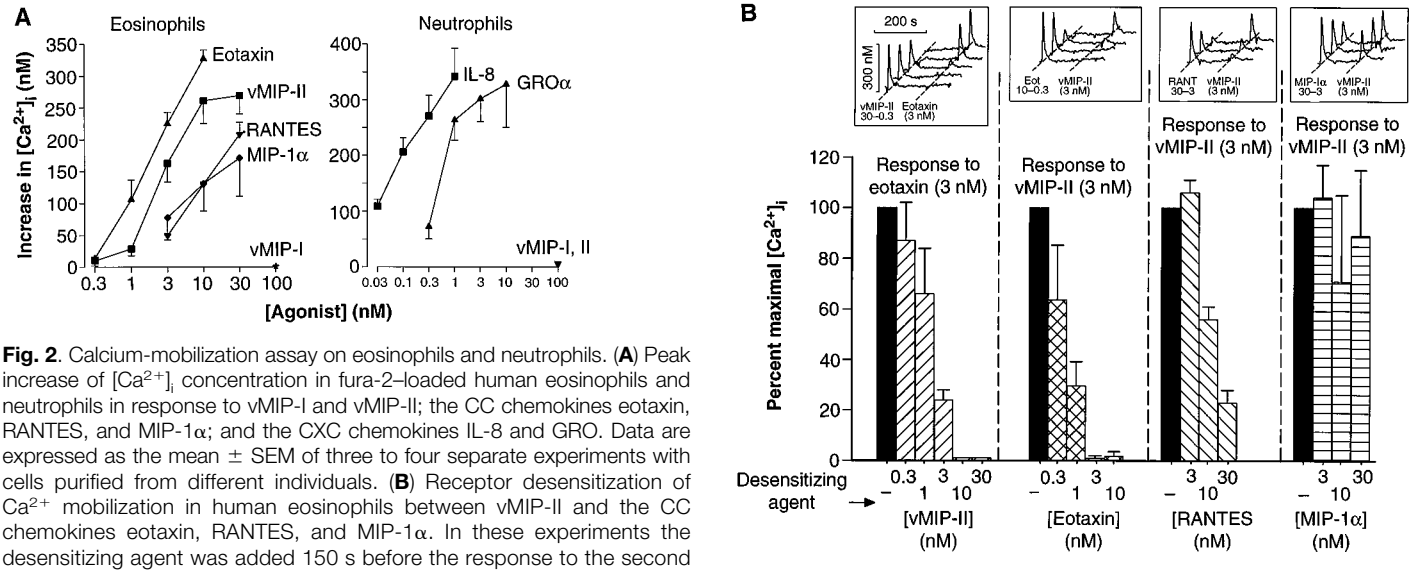

Fig. 2. Calcium-mobilization assay on eosinophils and neutrophils. (**A**) Peak increase of $[Ca^{2+}]_i$ concentration in fura-2–loaded human eosinophils and neutrophils in response to vMIP-I and vMIP-II; the CC chemokines eotaxin, RANTES, and MIP-1α; and the CXC chemokines IL-8 and GRO. Data are expressed as the mean ± SEM of three to four separate experiments with cells purified from different individuals. (**B**) Receptor desensitization of Ca^{2+} mobilization in human eosinophils between vMIP-II and the CC chemokines eotaxin, RANTES, and MIP-1α. In these experiments the desensitizing agent was added 150 s before the response to the second agonist was measured. Data are expressed as the percentage of the maximal $[Ca^{2+}]_i$induced by vMIP-II (3 nM) or eotaxin (3 nM) alone (filled columns) after treatment of the cells with various concentrations of the desensitizing agent (vMIP-II, 0.3 to 30 nM; eotaxin, 0.3 to 10 nM; RANTES, 3 to 30 nM; and MIP-1α, 3 to 30 nM). Values are the mean ± SEM of three separate experiments with eosinophils purified from different individuals. (Insets) Representative traces of the data from a single experiment showing the dose-response relation between the magnitude of the response to the desensitizing agent and the subsequent response to the second agonist. The desensitization was specific rather than global because none of the desensitizing agents reduced the response of the cells to a subsequent addition of the complement fragment C5a.

phils to eotaxin, and neither vMIP-I nor vMIP-II prevented Ca^{2+} mobilization in neutrophils induced by IL-8 (data not shown).

Whereas CCR3 is the predominant chemokine receptor through which eotaxin, RANTES, and other CC chemokines activate eosinophils (*18*), RANTES and MIP-1α can use CCR1 (*21*), which is also expressed on eosinophils. To determine the receptor usage by vMIP-II on eosinophils, we performed desensitization studies. vMIP-II exhibited complete cross-desensitization with eotaxin, partial desensitization with RANTES, and no desensitization with MIP-1α (Fig. 2B), providing functional evidence that vMIP-II binds to CCR3 on eosinophils.

To show that vMIP-II can chemoattract eosinophils, we performed an in vitro chemotaxis assay (*22*). vMIP-II, but not vMIP-I, was chemotactic for human eosinophils (Fig. 3). This activity of vMIP-II was comparable to that of eotaxin, which correlates with the activity to induce Ca^{2+} mobilization (Fig. 2A).

Although angiogenesis is central in the pathology of KS and prominent in MCD, the mechanisms by which KSHV induces new blood vessel formation are not known. Angiogenesis is a complex process involving chemotactic migration and proliferation of endothelial cells, followed by lumen formation and functional maturation of the endothelium (*23*). Often it is associated with the presence of activated inflammatory cells. Apart from their potent biological effects on leukocytes, some members of the chemokine family have been shown to have a direct effect on blood vessel formation. Within the CXC chemokine family, proteins containing the NH_2-terminal Glu-Leu-Arg (ELR) amino acid sequence motif such as IL-8 are angiogenic factors, whereas non–ELR-containing proteins including IP-10 are angiostatic (*24*). To our knowledge, there is no information on the angiogenic ability of CC chemokines. We therefore examined the potential of vMIP-I and vMIP-II as mediators of angiogenesis in the chick chorioallantoic membrane (CAM), which is a standard in ovo assay to investigate angiogenic function (*25*, *26*).

Angiogenic responses were observed and photographed 3 days after implantation of a methylcellulose disk containing test samples onto CAM. Most eggs implanted with vMIP-I or vMIP-II showed a clear angiogenic response. The positive controls used, vascular endothelial growth factor (VEGF) and phorbol 12-myristate 13-acetate (TPA), also induced angiogenesis as expected (Fig. 4 and Table 1). In contrast, cellular MIP-1α and RANTES failed to induce angiogenesis in most eggs, and the few positive responses recorded were not as prominent as those for vMIPs. The potency of vMIPs to induce angiogenesis in chick embryos was demonstrated by clear angiogenic responses in some eggs at doses as low as 0.05 μg, in contrast to poor induction by human CC chemokines at 0.25 μg. Although it is difficult to interpret a comparison of angiogenic activity between chemically synthesized and recombinant proteins, the activity of the vMIPs was not as potent as that of VEGF, but more potent in the CAM assay than that of the ELR-CXC chemokine IL-8 (Table 1). Preliminary results also indicate that eotaxin is not an inducer of angiogenesis in CAM. The finding that KSHV-encoded chemokines can induce new blood vessel formation in the chick CAM is intriguing and could have important implications for the role of KSHV in KS and MCD development.

Our results demonstrate that the vMIPs are biologically active: (i) vMIP-II binds predominantly to CCR3, resulting in potent inhibition of HIV entry by way of this receptor and activation and chemotaxis of

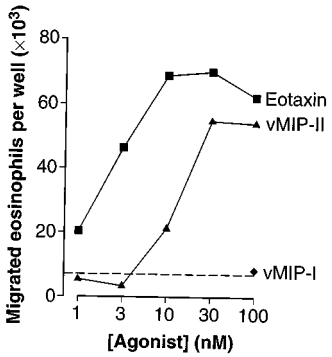

Fig. 3. Human eosinophil transwell chemotaxis assay. vMIP-II and eotaxin are chemotactic for human eosinophils in vitro. vMIP-I shows no activity in this assay. Buffer alone is represented by a dashed line.

Table 1. Angiogenic effect of vMIPs on the chick CAM.

Sample*	Dose (μg)	Number of embryos	Angiogenic response†			Score‡	Percent maximum score
			+	±	–		
vMIP-I	2.0	9	6	3	0	7.5	83
	1.0	9	8	1	0	8.5	94
	0.5	6	4	0	2	4	67
	0.25	25	13	4	8	15	60
	0.05	17	4	9	4	8.5	50
	0.01	9	2	2	5	3	33
vMIP-II	2.0	7	4	3	0	5.5	79
	1.0	10	6	3	1	7.5	75
	0.5	8	4	3	1	5.5	69
	0.25	24	8	12	4	14	58
	0.05	18	7	5	6	9.5	53
	0.01	8	0	4	4	2	25
hMIP-1α	0.25	9	0	2	7	1	11
RANTES	0.25	8	1	2	5	2	25
VEGF	0.5	7	7	0	0	7	100
	0.25	6	3	3	0	4.5	75
IL-8§	1.0	9	1	3	5	2.5	28
	0.25	7	0	2	5	1	14
TPA	0.08	7	7	0	0	7	100
BSA	20	8	0	0	8	0	0
H_2O	–	23	0	2	21	1	4

*Angiogenesis induction was performed by a methylcellulose disk containing synthetically prepared vMIP-I, vMIP-II, human MIP-1α, and RANTES. VEGF and TPA were used as positive controls. A disk containing vehicle only or 20 μg of BSA was used as a negative control. †Angiogenic responses were judged by three investigators: (+) unanimously positive; (±) unclear or split judgment; (–) unanimously negative. ‡Scores of 1, 0.5, and 0 were counted for (+), (±), and (–) results, respectively. Percent maximum score is the division of the score by the embryo number. §A CXC ELR-containing chemokine.

eosinophils. (ii) vMIP-II also exhibits weak HIV inhibition through other chemokine receptors. (iii) Both vMIPs induce angiogenesis in chick embryos. These activities may have important implications in viral pathogenesis. vMIP-I and vMIP-II inhibit HIV replication in PBMCs, albeit modestly. In patients with high KSHV viral load, especially as seen in the lymph nodes of HIV-positive individuals (*10*), these viral chemokines may affect HIV pathogenesis. vMIP-II inhibition of HIV infection by way of CCR3 is potent. This result is consistent with the report in which only vMIP-II was studied with a single HIV-1 strain (*27*). CCR3 is one of the main receptors for HIV-1 entry into microglia, and an antibody to CCR3 can inhibit HIV-1 infection of microglia (*28*). Patients with KS or high KSHV viral load, or both, may be less likely to develop HIV-related dementias. The potent agonistic activity of vMIP-II for eosinophils contrasts with its antagonistic function shown in other cell systems (*27*). Although previous studies have shown that HIV Tat is angiogenic (*2*), this protein does not play a role in the pathogenesis of non-AIDS KS (for example, classic, African endemic, and posttransplant KS). In contrast, KSHV is present at high levels in all epidemiologic types of KS, and the demonstration of angiogenesis induced by these viral-encoded proteins is the first in vivo indication that KSHV-encoded proteins have the potential to directly induce angiogenesis. Although it is unlikely that these viral chemokines are solely responsible for the marked vascularity seen in KSHV-associated tumors, they could contribute with other angiogenic factors involved in KS spindle cell growth or MCD development—for example, VEGF, basic fibroblast growth factor and IL-6 (*2*, *29*).

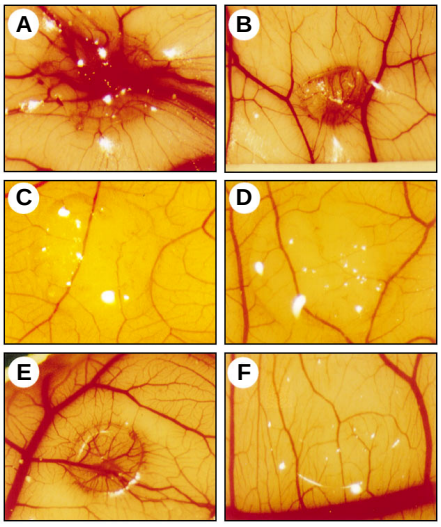

Fig. 4. Induction of angiogenesis by vMIPs in chick CAM. Methylcellulose discs containing vMIP-I (**A**), vMIP-II (**B**), RANTES (**C**), MIP-1α (**D**), VEGF (**E**), and BSA (**F**) were implanted onto 10- or 11-day-old CAMs. Photographs were taken 3 days later. Representative samples are shown.

REFERENCES AND NOTES

1. V. Beral, in *Cancer, HIV and AIDS*, V. Beral, H. W. Jaffe, R. A. Weiss, Eds. (Cold Spring Harbor Laboratory Press, Cold Spring Harbor, NY, 1991), vol. **10**, pp. 5–22; A. Wahman, S. L. Melnick, F. S. Rhame, J. D. Potter, *Epidemiol. Rev*. **13**, 178 (1991).
2. B. Ensoli, G. Barillari, S. Z. Salahuddin, R. C. Gallo, S. F. Wong, *Nature* **345**, 84 (1990); B. Ensoli *et al*., *ibid.* **371**, 674 (1994); A. Albini *et al*., *Nature Med.* **2**, 1371 (1996).
3. Y. Chang *et al*., *Science* **266**, 1865 (1994); C. Boshoff *et al*., *Lancet* **345**, 761 (1995); D. H. Kedes *et al*., *Nature Med.* **2**, 918 (1996); S. J. Gao *et al*., *ibid.*, p. 925 ; E. T. Lennette *et al*., *Lancet* **348**, 858 (1996); G. R. Simpson *et al*., *ibid.*, p. 1133.
4. V. Beral, T. A. Peterman, R. L. Berkelman, H. W. Jaffe, *Lancet* **335**, 123 (1990).
5. C. Boshoff *et al*., *Nature Med.* **1**, 1274 (1995); K. A. Staskus *et al*., *J. Virol.* **71**, 715 (1997).
6. J. M. Orenstein *et al*., *J. Acquired Immun. Defic. Syndr.* **11**, 735 (1997).
7. Although only the minority of cells in KS lesions at a specific time point undergo lytic replication [K. A. Staskus *et al*., *J. Virol.* **71**, 715 (1997)], the demonstration that hundreds of virions are produced in such cells (*6*) indicates that high local levels of lytic KSHV-encoded proteins are produced in KS lesions. Our analysis by reverse transcriptase–polymerase chain reaction showed expression of vMIP-I and vMIP-II mRNA in KS biopsies (*30*).
8. J. Soulier *et al*., *Blood* **86**, 1276 (1995); N. Dupin *et al*., *N. Engl. J. Med*. **333**, 798 (1996); A. Gessain *et al*., *Blood* **87**, 414 (1996); A. Chadburn *et al*., *Cancer* **80**, 788 (1997); C. Parravicini *et al.*, *Am. J. Pathol.*, in press.
9. J. J. Russo *et al*., *Proc. Natl. Acad. Sci. U.S.A.* **93**, 14862 (1996).
10. P. S. Moore, C. Boshoff, R. A. Weiss, Y. Chang, *Science* **274**, 1739 (1996).
11. F. Neipel, J.-C. Albrecht, B. Fleckenstein, *J. Virol.* **71**, 4187 (1997).
12. C. R. Mackay, *J. Exp. Med.* **184**, 799 (1996); D. H. Adams, A. R. Lloyd, *Lancet* **349**, 490 (1997).
13. F. Cocchi *et al*., *Science* **270**, 1811 (1995); T. Dragic *et al*., *Nature* **381**, 667 (1996); H. Deng *et al*., *ibid.*, p. 661; G. Alkhatib *et al*., *Science* **272**, 1955 (1996); H. Choe *et al*., *Cell* **85**, 1135 (1996); P. M. Murphy, *Nature* **385**, 296 (1997).
14. Synthetic chemokines were generated by native chemical ligation of peptides synthesized by solid-phase methods on an Applied Biosystems 430A Peptide Synthesizer [P. E. Dawson, T. W. Muir, I. Clark-Lewis, S. B. H. Kent, *Science* **266**, 776 (1994)]. The resulting chemokines were purified by reversed-phase high-performance liquid chromatography and characterized by electrospray mass spectrometry. The purified synthetic chemokines were reconstituted in phosphate-buffered saline (PBS), and samples were frozen at −70°C. Chemokine sequences correspond to amino acid residues 25 to 29 for vMIP-1 and 21 to 94 for vMIP-II (GenBank accession number U75698).
15. PBMCs were isolated as described (*31*). They were stimulated with phytohemagglutinin (PHA, 0.5 μg/ml) and cultured for 2 to 3 days before addition of IL-2 (Boehringer Mannheim, 20 U/ml). SL-2 and SF162 viruses are NSI, macrophage-tropic HIV-1 strains that use CCR5 as a coreceptor (*31*). Strains 89.6 and 2028 are SI, dual-tropic strains that use CXCR-4, CCR5, and CCR3 (*31*). Strain 89.6 can also use CCR2b [B. J. Doranz *et al*., *Cell* **85**, 1149 (1996)]. Virus stocks were produced in PHA–IL-2–stimulated PBMCs. ROD/B is a variant of HIV-2 ROD strain that efficiently infects CD4-negative/CXCR4$^+$ cells (*16*). Virus stocks were produced in H9 cells. For chemokine inhibition, 7.5×10^4 PBMCs were treated with appropriate concentrations of chemokines in 50 μl for 30 min at 37°C. Virus (1000 median tissue culture infectious dose in 50 μl) was added and incubated at 37°C for 3 hours. Cells were then washed four times and resuspended in 150 μl of media containing IL-2 and relevant chemokine at the appropriate concentration. Cells were fed every 3 days with fresh medium contain-

ing IL-2 and chemokine. Supernatants were harvested on day 9 and assayed for p24 levels.On U87/CD4 cells, virus infectivity was assessed by a focus-forming assay as described [G. Simmons *et al*., *Science* **276,** 276 (1997)]. Briefly, for viruses using more than one coreceptor, focus-forming units (FFUs) were assessed separately for each appropriate coreceptor expressing U87/CD4 cell type. Cells were seeded into 48-well trays at 1×10^4 cells per well overnight. The cells were then treated for 30 min at 37°C with appropriate concentrations of chemokine in 75 μl. One hundred FFUs of each virus in 75 μl were added and incubated for 3 hours at 37°C. The cells were then washed three times, and 500 μl of medium containing the appropriate chemokine at the correct concentration was added. After 5 days the cells were fixed for 10 min in cold acetone:methanol (1:1) and immunostained for in situ p24 as described [Á. McKnight, P. R. Clapham, R. A. Weiss, *Virology* **201**, 8 (1994)]. Standard errors were estimated from duplicate wells, and the results (Fig. 1) are representative of three separate experiments.
16. M. J. Endres *et al*., *Cell* **87**, 745 (1996); J. D. Reeves *et al*., *Virology* **231**, 130 (1997).
17. Neither RANTES, vMIP-I, nor vMIP-II had appreciable effect on SF162 infection of U87/CD4 CCR5 cells, whereas vMIP-II and vMIP-I blocked infection by SL-2 at 400 nM by more than 50 and 25%, respectively. vMIP-II, but not vMIP-I, blocked the SI strains 89.6 and 2028 at 200 nM by 50 and 20%, respectively, compared with RANTES, which blocked infection of these viruses completely at 100 nM. On U87/CD4 CXCR4 cells, both vMIP-I and vMIP-II showed little activity (10 to 30% inhibition at 200 nM) in blocking infection by strain 89.6 or 2028. On U87 CXCR4 cells (CD4 negative), inhibition of infection by HIV-2 ROD/B was ~50% at 200 nM by vMIP-I and vMIP-II.
18. P. D. Ponath *et al*., *J. Exp. Med.* **183**, 2437 (1996); B. L. Daugherty *et al*., *ibid.*, p. 2349.
19. Human eosinophils and neutrophils were isolated from the peripheral blood of healthy volunteers as described [P. J. Jose *et al*., *J. Exp. Med.* **179**, 881 (1994)]. Briefly, neutrophils (>95% purity, contaminating cells being a mixture of eosinophils and mononuclear cells) were separated from red blood cells and mononuclear cells by sequential dextran sedimentation and Percoll–plasma density centrifugation. Eosinophils (>98% purity, contaminating cells being mononuclear cells) were isolated from healthy atopic individuals as described above for neutrophils followed by immunomagnetic separation of the eosinophils from the neutrophils with anti-CD16 microbeads as described (*32*). Calcium mobilization in purified neutrophils and eosinophils was measured as described (*32*). Briefly, purified neutrophils or eosinophils were incubated with fura-2 acetoxy-methyl ester (1 to 2.5 μM), washed three times in 10 mM PBS (without Ca^{2+} or Mg^{2+}) + 0.1% bovine serum albumin (BSA) (200*g*, 8 min), and resuspended at 2×10^6 cells/ml in 10 mM PBS (without Ca^{2+} or Mg^{2+}) + 0.25% BSA + 10 mM Hepes + 10 mM glucose. Aliquots of cells were placed in quartz cuvettes, and the external Ca^{2+} concentration was adjusted to 1 mM with $CaCl_2$. Changes in fluorescence were measured at 37°C by means of a fluorescence spectrophotometer at excitation wavelengths of 340 and 380 nm and an emission wavelength 510 nm. Intracellular Ca^{2+} concentration $[Ca^{2+}]_i$ was calculated with the ratio of the two fluorescence readings and a dissociation constant for Ca^{2+} at 37°C of 224 nM. In experiments designed to investigate desensitization between agonists, the first agonist (the desensitizing agonist) was added after 50 s and the second agonist added 150 s later.
20. A. E. I. Proudfoot *et al*., *J. Biol. Chem.* **271**, 2599 (1996); B. Moser *et al*., *ibid.* **268**, 7125 (1993).
21. K. Neote, D. DiGregorio, J. Y. Mak, R. Horuk, T. J. Schall, *Cell* **72**, 415 (1993); J. L. Gao *et al*., *J. Exp. Med.* **177**, 1421 (1993).
22. Human eosinophils (5×10^5 cells/100 μl per well) were placed in 3-μm pore size transwell inserts and placed in cell culture wells containing 400 μl of human eotaxin, vMIP-I, or vMIP-II at various concentrations of buffer [RPMI 1640 + L-glutamine + 2% fetal calf serum + 10 mM Hepes (pH 7.4)] as described [P. D. Ponath *et al*., *J. Exp. Med.* **183**, 2437 (1996)]. After incubation at 37°C for 60 min (95% O_2, 5% CO_2), eosinophils migrating through the transwell were counted on a FACScan flow cytometer (Becton Dickinson).
23. W. Risau, *Nature* **387**, 671 (1997).
24. A. L. Angiolillo, C. Sgadari, G. Tosato, *Ann. N.Y. Acad. Sci.* **795**, 158 (1996); R. M. Strieter *et al*., *J. Biol. Chem.* **270**, 27348 (1995); Y. Cao, C. Chen, J. A. Weatherbee, M. Tsang, J. Folkman, *J. Exp. Med*. **182**, 2069 (1995).
25. D. Knighton, D. Ausprunk, D. Tapper, J. Folkman, *Br. J. Cancer* **35**, 347 (1977); P. C. Brooks, R. A. F. Clark, D. A. Cheresh, *Science* **264**, 569 (1994); M. Friedlander *et al*., *ibid*. **270**, 1500 (1995).
26. Angiogenic activities of synthetically prepared viral and human chemokines were evaluated by the chick CAM assay as described [T. Oikawa *et al*., *Cancer Lett*. **59**, 57 (1991)]. Fertilized Plymouth Rock × White Leghorn eggs were incubated at 37°C in a humidified atmosphere (relative humidity, ~70%). Test samples were dissolved in sterile distilled water or PBS. Sterilized sample solution was mixed with an equal volume of autoclaved 2% methylcellulose. Controls were prepared with vehicle only (1% methylcellulose solution). The sample solution (20 μl) was dropped on Parafilm and dried up. The methylcellulose disks were stripped off from the Parafilm and placed on a CAM of 10- or 11-day-old chick embryos. After 3 days, the CAMs were observed by means of an Olympus stereoscope. A 20% fat emulsion (Intralipos 20%, Midori-Juji, Osaka, Japan) was injected into the CAM to increase the contrast between blood and surrounding tissues [R. Danesi *et al*., *Clin. Cancer Res.* **3**, 265 (1997)]. The CAMs were photographed for evaluation of angiogenic response. Angiogenic responses were graded independently by three investigators as negative, positive, or unclear on the basis of infiltration of blood vessels into the area of the implanted methylcellulose.
27. T. Kledal *et al*., *Science* **277**, 1656 (1997).
28. J. He *et al*., *Nature* **385**, 645 (1997).
29. S. A. Miles *et al*., *Proc. Natl. Acad. Sci. U.S.A.* **87**, 4068 (1990); K. Yoshizaki *et al*., *Blood* **74**, 1360 (1989); K. Weindel, D. Marme, H. A. Weich, *Biochem. Biophys. Res. Commun.* **183,** 1167(1992); R. Masood *et al*., *Proc. Natl. Acad. Sci. U.S.A.* **94,** 979 (1997).
30. C. Boshoff *et al*., unpublished data.
31. G. Simmons *et al*., *J. Virol.* **70**, 8355 (1996).
32. P. J. Jose *et al*., *J. Exp. Med.* **179,** 881 (1994).
33. We thank D. Littman and J Hoxie for providing U87/CD4 cells, and P. Clapham and G. Simmons for doing HIV-1 experiments. Supported by the Cancer Research Campaign; the Medical Research Council; the Japanese Ministry of Health and Welfare; the Japanese Ministry of Education, Sciences, Sports and Culture; the Wellcome Trust; The National Asthma Campaign; and NCI (CA 67391).

1 July 1997; accepted 2 September 1997

Caspase-3–Generated Fragment of Gelsolin: Effector of Morphological Change in Apoptosis

Srinivas Kothakota,* Toshifumi Azuma,* Christoph Reinhard, Anke Klippel, Jay Tang, Keting Chu, Thomas J. McGarry, Marc W. Kirschner, Kirston Koths, David J. Kwiatkowski,† Lewis T. Williams

The caspase-3 (CPP32, apopain, YAMA) family of cysteinyl proteases has been implicated as key mediators of apoptosis in mammalian cells. Gelsolin was identified as a substrate for caspase-3 by screening the translation products of small complementary DNA pools for sensitivity to cleavage by caspase-3. Gelsolin was cleaved in vivo in a caspase-dependent manner in cells stimulated by Fas. Caspase-cleaved gelsolin severed actin filaments in vitro in a Ca^{2+}-independent manner. Expression of the gelsolin cleavage product in multiple cell types caused the cells to round up, detach from the plate, and undergo nuclear fragmentation. Neutrophils isolated from mice lacking gelsolin had delayed onset of both blebbing and DNA fragmentation, following apoptosis induction, compared with wild-type neutrophils. Thus, cleaved gelsolin may be one physiological effector of morphologic change during apoptosis.

A conserved family of aspartate-specific cysteinyl proteases (caspases) has been identified as critical mediators of apoptosis in *Caenorhabditis elegans* and mammals (*1*, *2*). Although multiple protein substrates of caspases have been found, the functional significance of the substrates is poorly understood (*3*). We reasoned that an unbiased approach to determine proteins that were the best substrates of caspase-3 in vitro would yield a physiologically relevant substrate. Therefore, we constructed a protein library by translating a murine embryo cDNA library in vitro (*4*) and tested the translated proteins for their sensitivity to caspase-3 cleavage. To facilitate screening, we separated the cDNAs into small pools before in vitro translation and incorporated [^{35}S]methionine into the translation mix to

S. Kothakota, C. Reinhard, A. Klippel, K. Chu, K. Koths, L. T. Williams, Chiron Corporation, Emeryville, CA 94608, USA.
T. Azuma, J. Tang, D. J. Kwiatkowski, Division of Experimental Medicine, Brigham and Women's Hospital, Boston, MA 02115, USA.
T. J. McGarry and M. W. Kirschner, Department of Cell Biology, Harvard Medical School, Boston, MA 02115, USA.

*These authors contributed equally to this work.
†To whom correspondence should be addressed. E-mail: kwiatkowski@calvin.bwh.harvard.edu

Angiogenic and HIV-Inhibitory Functions of KSHV-Encoded Chemokines

Chris Boshoff, Yoshio Endo, Paul D. Collins, Yasuhiro Takeuchi, Jacqueline D. Reeves, Vicki L. Schweickart, Michael A. Siani, Takuma Sasaki, Timothy J. Williams, Patrick W. Gray, Patrick S. Moore, Yuan Chang and Robin A. Weiss

Science **278** (5336), 290-294.
DOI: 10.1126/science.278.5336.290